

Nanodomain engineering in RbTiOPO_4 ferroelectric crystals

G. Rosenman,^{a)} P. Urenski, A. Agronin, A. Arie, and Y. Rosenwaks^{b)}

Department of Electrical Engineering-Physical Electronics, Tel Aviv University, Ramat-Aviv, 69978, Israel

(Received 6 January 2003; accepted 7 April 2003)

A high voltage atomic force microscope has been applied for tailoring strip-like nanodomains in RbTiOPO_4 ferroelectric crystal. Highly anisotropic nanodomain propagation has been observed owing to the difference in lattice constants along the principal axes of the RbTiOPO_4 crystal. Studying the influence of the applied high voltage, and tip velocity on the domain strips has allowed us to fabricate fine nanodomain gratings, which is useful for backward-propagating quasi-phase-matched frequency conversion. © 2003 American Institute of Physics.
[DOI: 10.1063/1.1578693]

The recently developed electrical poling method has enabled us to fabricate engineered domain superlattices (periodic, quasiperiodic, aperiodic, multiperiodic, etc.) in ferroelectric (FE) crystals in the micrometer scale. Such structures have allowed us to generate coherent light at any wavelength within the FE crystal transparency, and to develop tunable laser sources in a wide spectral region where compact and efficient lasers are unavailable.^{1,2}

To date, FE domain gratings fabricated using various methods have poling periods not less than $4 \mu\text{m}$.^{1,2} Much denser gratings, with a period of $1 \mu\text{m}$, enable one to efficiently convert light into the ultraviolet range. As an example, in order to generate 300-nm radiation by first-order quasi-phase-matching in periodically poled LiTaO_3 , the required domain width is $\sim 0.7 \mu\text{m}$. Furthermore, dense poling periods will allow us to obtain a specific class of nonlinear frequency conversion devices in which the generated wave propagates in the opposite direction to the input waves. Examples of backward-propagating frequency converters include backward propagating frequency doublers, and mirrorless backward optical parametric oscillators.³

Submicron and nanometer scale domains may be fabricated using atomic force microscopy (AFM)-based techniques. Data on the application of AFM for domain switching in FE crystals is limited.⁴⁻⁷ Several attempts were undertaken for direct domain writing in bulk FE crystals hundreds of micrometers thick. No domain growth throughout the crystal bulk was observed; in most cases, the domains were very unstable and disappeared a short time (several minutes to several days) following their formation.⁷⁻⁹ A breakthrough in the field emerged with the recent development of the high voltage atomic force microscope (HVAFM).¹⁰ Diverse stable domain configurations (one-dimensional and two-dimensional) were fabricated in several FE crystals.¹¹ As an example two-dimensional strip-domains 500 nm wide were tailored in LiNbO_3 crystal by applying 3.4-kV repolarization voltage. Application of kilovolts in the HVAFM generates at the apex of the tip a high electric field reaching 10^7 V/cm . Such a large field leads to drastic changes of the polarization reversal mechanism¹² that allows

us to form submicrometer-wide and several-hundred-micrometer-deep domains.^{10,11}

In this letter, we present a detailed study of domain reversal in RbTiOPO_4 (RTP) FE crystals using the scanning tip of the HVAFM. It is shown that sidewise nanodomain propagation in RTP crystals is highly anisotropic, and the growing domains strongly elongate along the Y axis. Studies of this phenomenon allowed us to find the optimal conditions for high accuracy fabrication of engineered nanodomain superlattices for nonlinear optical converters.

RbTiOPO_4 (RTP) crystals thinned down to $200\text{--}350 \mu\text{m}$ grown by the flux technique (Raicol Crystals, Ltd, Israel) were used. The samples were cut normal to the Z crystallographic polar axis and thoroughly polished. The HVAFM is based on a modification of the Autoprobe CP AFM (Veeco, Inc).¹¹ The gratings were tailored by applying a high dc voltage to the scanning HVAFM tip; a heavily boron-doped silicon cantilever with a tip having a radius of curvature of 50 nm was used. After an appropriate commutation, the HVAFM was employed in the conventional electrostatic contact mode for imaging of the tailored domain structures.¹³ The fabricated domains were also inspected, following chemical etching, using optical microscopy.

Figure 1 shows optical microscopy image of the C^+ polar face of the periodic domain configuration fabricated in a $200\text{-}\mu\text{m}$ -thick RTP crystal. The domains were obtained using

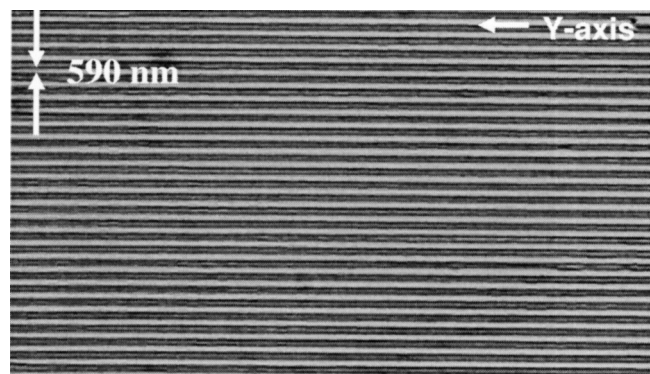


FIG. 1. Optical microscopy image of the C^+ polar face of the periodic domain structure fabricated in a $200\text{-}\mu\text{m}$ -thick RTP sample where HVAFM tip scanning was performed along the Y -axis direction (after selective etching).

^{a)}Electronic mail: gilr@eng.tau.ac.il

^{b)}Electronic mail: yossir@eng.tau.ac.il

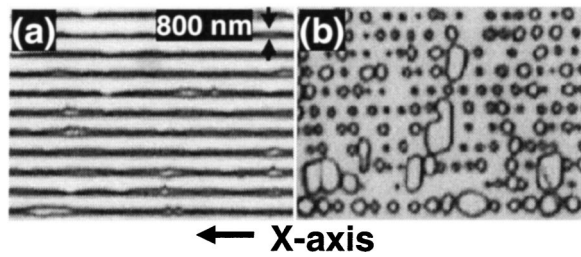


FIG. 2. Optical microscopy image of domain structure fabricated in the RTP sample when HVAFM tip scanning was performed along the X -axis direction: (a) C^+ polar face; (b) C^- polar face (after selective etching).

an applied voltage of 650 V and a tip velocity of 30 $\mu\text{m/s}$. The structure was fabricated with a tip scanning direction coinciding with the Y principal axis of the RTP crystal. The reversed domain strips were 590 nm wide, and the domain walls were smooth along the Y axis. Insignificant variation of the periodicity of the domain grating was found on the opposite C^- polar face, indicating that the reversed domains propagate perfectly without any change in width throughout the crystal from the C^+ to the C^- polar face.

Figure 2 shows optical images of the strip-like nanodomain structure fabricated in the same RTP plate when the HVAFM tip direction scanning was performed along the crystal X axis, under identical experimental conditions ($V = 650$ V, scanning velocity 30 $\mu\text{m/s}$). The domain strips are quasihomogeneous on the C^+ -polar face [Fig. 2(a)], while on the C^- face [Fig. 2(b)], the domain structure consists of isolated separated domains located along the scanning X -line [Fig. 2(b)]. Most of the reversed domains that propagated throughout the crystal bulk are elongated along the Y axis. Some domains grew to the big islands crossing the sample with preferable orientation in the Y direction. Thus, the HVAFM tip scanning along the X axis gave rise to nanodomain growth and coalescence along the Y axis producing both discontinuity of the domain grating and strong domain widening on the C^- face [Fig. 2(b)].

The polarization reversal in ferroelectrics is a multistage process that includes several stages: nucleation of new domains with opposite direction of spontaneous polarization, its forward growth into the FE crystal bulk, and sidewise motion of the domain walls. It was recently found that removing the applied switching field is followed by the fourth stage stabilization of the reversed domains.¹⁴ The first three stages strongly depend on the applied switching electric field. The previously proposed models of domain nucleation,^{15–18} forward growth,¹⁹ and sidewise motion of the domain walls²⁰ were developed for switching fields in the range of 10^3 to 10^5 V/cm. These previous studies of the different stages of the domain reversal were performed under homogeneous electric field,^{14–20} such a field distribution is found in the conventional setup using uniform plain switching electrodes.

Application of high voltage to the sharp tip of the HVAFM generates a very strong switching field. The normal component of this field E_z can be calculated using Eq. (1) reported by us recently:¹¹

$$E_z(z) = \frac{2q}{(\sqrt{\epsilon_c \epsilon_a} + 1)} \sqrt{\frac{\epsilon_a}{\epsilon_c}} \frac{R + \delta + z \sqrt{\epsilon_a / \epsilon_c}}{[\epsilon_c (R + \delta + z \sqrt{\epsilon_a / \epsilon_c})^2 + \rho^2]^{3/2}}, \quad (1)$$

where q is the tip charge induced by the external voltage,¹¹ δ is the distance from the tip apex to the sample surface, ρ is the distance along the surface from the point of the tip apex projection on the sample surface, z is the distance from the sample surface to the bulk along the Z polar axis, and ϵ_c and ϵ_a are the dielectric constants in the polar and nonpolar direction, respectively. Substitution of the experimental parameters in the present study [$V = 650$ V, tip radius of curvature $R = 50$ nm, $\epsilon_c = 25$, $\epsilon_a = 18$ (Ref. 21)], gives for the field at the apex of the tip ($\delta \sim 0.1$ nm) a field of $E \sim 10^7$ V/cm. This field is larger by two to three orders of magnitude than conventionally applied repolarization fields.^{1,2,14–18,20} Such a large field leads to almost zero activation energy for domain nucleation, quasiatomic nucleus dimensions, and very short nucleation time, close to the period of lattice vibrations.¹²

The most distinguishing feature of the polarization reversal in HVAFM is the strongly inhomogeneous distribution of the field generated by the needle-like AFM tip. Our calculations using Eq. (1) show that the applied switching field decreases rapidly from the surface ($E \sim 10^7$ V/cm) to the crystal bulk, and at a depth of about 50 μm , the field does not exceed a few V/cm. Despite this negligibly small electric field in the crystal bulk, the nucleated domains propagate through the entire crystal thickness (Figs. 1 and 2). Some of the domains have a radius of around $r \sim 100$ nm [Fig. 2(b)], which is three orders of magnitude smaller than the crystal thickness l . This phenomenon of string-like domain formation, which was given the name “domain breakdown” is described in detail in Ref. 12.

The data in this study show that most of the inverted nanodomains reaching the opposite polar face have elliptical shape demonstrating preferable sidewise growth along the Y axis [Fig. 2(b)]. It may be assumed that the anisotropic growth of the nanodomains along the Y axis prevents domain coalescence in the X direction, leading to discontinuity of the domain strips when the scanning occurs along the X crystal axis.

These observed peculiarities of the nanodomain growth occur at the third stage of the domain reversal sidewise domain wall motion. The theory proposed for this stage²⁰ considers the wall motion as repeated nucleation of steps along the existing 180° domain wall. The rate of nucleation is proportional to $\sim \exp(-\Delta U_a/kT)$, where $\Delta U_a = kT \delta_t / E$ is the activation energy for domain nucleation at the wall, and δ_t is the activation field of a FE crystal.²¹ Our previous studies of polarization reversal in KTiOPO_4 crystals, which are isomorphic to RTP, allowed us to obtain the value of the activation fields $\delta_t = 1.12 \times 10^5$ V/cm.²² Our calculation of the activation energy under strong electric field $E \sim 10^7$ V/cm generated at the apex of the AFM tip, showed that the activation energy of the domain nuclei at the wall is $\Delta U_a = 4 \times 10^{-4}$ eV,¹² and therefore a very high nucleation rate in the vicinity of the tip. This may cause a formation of numerous nuclei located at the growing domain wall, resulting in a very large domain wall velocity. It may be assumed that under the condition of this extremely high nucleation rate, the domain wall moves fast in a quasicontinuous manner as one unit, and its motion is isotropic [Figs. 1 and 2(a)]. Such domain wall motion under a very strong electric field and infinite nucleation rate is not described by the Miller and Weinreich

theory.²⁰ The later model was developed for the case of low electric fields when $\delta_i > E$, and it defines the velocity of the wall motion as²³

$$v = v_\infty \exp(-\delta_i/E - E_C), \quad (2)$$

where E_C is the coercive field. The coercive field measured for RTP crystals²⁴ is $E_C = 35 \times 10^3$ V/cm. Thus, the super-high field $E \sim 10^7$ V/cm generated by the HVAFM tip is by two orders of magnitude larger than the activation field δ_i , and it exceeds the coercive field E_C by four orders of magnitude. This may lead to a different physical mechanism of sidewise domain motion.

The field distribution calculated using Eq. (1) on the surface at the edge of the strip-domain, that is, at a distance ρ of around 290 nm from the tip is $\sim 1.5 \times 10^5$ V/cm which is close to the activation field δ_i . At a depth of around 10 μm below the surface, the field decreases to $E \sim 360$ V/cm, satisfying the condition $\delta_i > E$ which allows to apply the Miller–Weinreich model.²⁰ Considering the nucleation of triangular domain steps at the existing domain wall this model showed that preferable wall motion occurs in the direction where the activation field δ_i is minimum.²⁰ The equation obtained by Miller and Weinreich for the domain walls velocity may be written in the form²⁵

$$v = v_\infty \exp(-kb^{*3/2}), \quad (3)$$

where b^* is the minimum nucleation step in the wall motion direction (taken by Miller and Weinreich as one lattice constant), and k is a coefficient depending strongly on domain wall energy density $\sigma_w^{3/2}$. Analysis of Eq. (3) results in an exponential dependence of the domain velocity on both the wall motion direction b^* , and on the wall energy density σ_w

$$v \sim \exp(-b^*)^{3/2}, \quad v \sim \exp(-\sigma_w)^{3/2}. \quad (4)$$

There is no reported data on anisotropic properties of wall energy density σ_w . However if we compare the minimum steps b^* along the X and Y axes, which are the lattice constants a_x and a_y , we find that the RTP crystal lattice is highly distorted, $a_x = 12.96 \text{ \AA}$, $a_y = 6.49 \text{ \AA}$.²⁶ The lattice constant a_x is twice longer than a_y ; thus, in accordance with Eq. (4), the domain wall velocity along the Y axis will be at least one order of magnitude larger than that along the X axis, which is consistent with the observed anisotropic domain growth [Fig. 2(b)].

The sidewise domain wall motion in RTP crystals reversed using the HVAFM shows two different phenomena: isotropic domain growth under the super-high field in the vicinity of the AFM apex, and anisotropic wall propagation under low electric fields generated far from the tip due to the highly inhomogeneous field distribution. It should be noted that the difference in the lattice constants in KTP and family crystals is highly pronounced as compared to other ferroelectrics. This property allows us to choose such crystals for tailoring of high-resolution domain gratings both in the micrometer^{2,27} and the nanometer scale.

Systematic experiments were conducted for fabrication of domain gratings in RTP crystals by varying the applied voltage in the range from 500 to 900 V and the HVAFM tip scanning velocity in the 20–170- $\mu\text{m/s}$ range along the Y

axis. It was found that the width of the domain strips inverted under the moving switching electrode-HVAFM tip is strongly influenced by the tip velocity and the applied voltage. A larger tip velocity leads to narrower reversed domains; the width of the domain strips increases with applied voltage.

The results just described on the anisotropic domain propagation (Figs. 1 and 2), as well as on the dependence of the domain strips width on the applied voltage and the tip velocity, allowed us to find the optimal conditions for tailoring high-resolution periodically poled nanodomain configuration for a backward-propagating frequency converter. Figure 1 shows a nanodomain grating with a domain 590 nm wide, which will be used for eleventh-order backward quasi-phase-matched second-harmonic generation of 415-nm light. The 0.2×1 mm grating fabrication lasted 12 h. We believe that one of the possibilities to improve this nanotechnology should be done through the use of large AFM stages and/or multiple tip arrays.

The authors highly appreciate the support of the Israeli Ministry of Science Culture and Sport, and Nanoscience and Nanotechnology Center in Tel Aviv University and fruitful discussions with Prof. M. Molotskii.

¹L. M. Myers, R. C. Eckardt, M. M. Fejer, and R. L. Byer, *J. Opt. Soc. Am. B* **12**, 2102 (1995).

²G. Rosenman, A. Arie, and A. Skliar, *Ferroelectr. Rev.* **1**, 4 (1998).

³S. E. Harris, *Appl. Phys. Lett.* **9**, 114 (1966).

⁴K. Franke, J. Besold, W. Haessler, and C. Seege-barth, *Surf. Sci. Lett.* **302**, 283 (1994).

⁵A. Gruverman, O. Kolosov, J. Hatano, K. Takahashi, and H. Tokumoto, *J. Vac. Sci. Technol. B* **13**, 1095 (1995).

⁶L. M. Eng., M. Bammerlin, C. Loppacher, *et al.*, *Ferroelectrics* **222**, 421/163 (1999).

⁷L. M. Eng, H.-J. Guntherodt, G. Rosenman, A. Skliar, M. Oron, M. Katz, and D. Eger, *J. Appl. Phys.* **83**, 5973 (1998).

⁸L. M. Eng, M. Abplanalp, and P. Gunter, *Appl. Phys. A: Mater. Sci. Process.* **66**, S679 (1998).

⁹A. Gruverman, J. Hatano, and H. Tokumoto, *Jpn. J. Appl. Phys.* **36**, 2207 (1997).

¹⁰G. Rosenman, Y. Rosenwaks, and P. Urenski, Patent Pending, Submitted October, 2001.

¹¹G. Rosenman, P. Urenski, A. Agronin, Y. Rosenwaks, and M. Molotskii, *Appl. Phys. Lett.* **82**, 103 (2003).

¹²M. Molotskii, A. Agronin, P. Urenski, M. Shvebelman, G. Rosenman, and Y. Rosenwaks, *Phys. Rev. Lett.* **90**, 107601 (2003).

¹³M. Shvebelman, P. Urenski, R. Shikler, G. Rosenman, Y. Rosenwaks, and M. Molotskii, *Appl. Phys. Lett.* **80**, 1806 (2002).

¹⁴V. Gopalan, T. E. Mitchell, and K. E. Sicakfus, *Solid State Commun.* **109**, 111 (1999).

¹⁵W. Merz, *Phys. Rev.* **95**, 690 (1954).

¹⁶R. J. Landauer, *J. Appl. Phys.* **28**, 227 (1957).

¹⁷M. Molotskii, R. Kris, and G. Rosenman, *J. Appl. Phys.* **88**, 5318 (2000).

¹⁸A. M. Bratkovsky and A. P. Levanyuk, *Phys. Rev. Lett.* **85**, 4614 (2000).

¹⁹M. Molotskii, *Philos. Mag. Lett.* (to be published).

²⁰R. Miller and G. Weinreich, *Phys. Rev.* **117**, 1460 (1960).

²¹M. Wang, J. Y. Wang, Y. G. Liu, and J. Q. Wei, *Ferroelectrics* **15**, 13 (1991).

²²G. Rosenman, A. Skliar, M. Oron, and M. Katz, *J. Phys. D* **30**, 277 (1997).

²³S. Kim, V. Gopalan, K. Kitamura, and Y. Furukawa, *J. Appl. Phys.* **90**, 2949 (2001).

²⁴P. Urenski, G. Rosenman, and M. Molotskii, *J. Mater. Res.* **16**, 1493 (2001).

²⁵P. Urenski, M. Lesnykh, Y. Rosenwaks, G. Rosenman, and M. Molotskii, *J. Appl. Phys.* **90**, 1950 (2001).

²⁶L. K. Cheng and J. D. Bierlein, *Ferroelectrics* **142**, 209 (1993).

²⁷K. Fradkin-Kashi, A. Arie, P. Urenski, and G. Rosenman, *Phys. Rev. Lett.* **88**, 023903 (2002).